GEOLOGICA CARPATHICA, 52, 3, BRATISLAVA, JUNE 2001
127–138

PHYLLOSILICATES FROM HYDROTHERMALLY ALTERED GRANITOID ROCKS IN THE PEZINOK Sb-Au DEPOSIT, WESTERN CARPATHIANS, SLOVAKIA

DANIEL MORAVANSKÝ[1*], MARTIN CHOVAN[1] and JOZEF LIPKA[2]

[1]Department of Mineralogy and Petrology, Faculty of Science, Comenius University, Mlynská dolina, 842 15 Bratislava, Slovak Republic
[2]Department of Nuclear Physics and Technology, Slovak University of Technology, Ilkovičova 3, 812 19 Bratislava, Slovak Republic

(Manuscript received September 22, 2000; accepted in revised form March 15, 2001)

Abstract: Biotites from altered granitoid rocks on Pezinok-Kolársky vrch Hill Sb-Au deposit belong to the phlogophite-annite series with the ratio $Fe_{tot}/(Fe_{tot} + Mg)$ = 0.44–0.55. Mg-biotites are the dominant type and can be classified as phlogopites ($Phl_{30.09-45.79}Ann_{26.67-36.00}Eas_{22.93-10.22}Sid_{20.31-8.02}$). Fe-biotites (annites, $Phl_{34.79-41.13}Ann_{39.20-46.39}Eas_{12.22-5.86}Sid_{13.79-6.62}$) are present in the more altered rocks. The chemical composition of the studied biotites is governed by Tschermak's substitution, dioctahedral-trioctahedral substitution and $A_{-1}(Si_{+1}Al_{-1})^{IV}$-substitution. Interlayer deficient occupancy of A site is probably caused by postmagmatic hydrothermal alteration and can be explained by $A_{-1}(Si_{+1}Al_{-1})^{IV}$-substitution. The studied tri-trioctahedral chlorites come from the clinochlore-chamosite isomorphic series and they originated from biotites. According to the classification of Wiewióra & Weiss (1990) or Weiss (1991), they can be divided into two groups: ferrous clinochlores (schematic formula $Mg_{34.39-36.32}Fe_{28.31-37.07}X_{24.02-35.39}$) and magnesium chamosites (schematic formula $Mg_{34.33-37.90}Fe_{34.76-39.32}X_{23.18-28.30}$). Ferrous clinochlore is the dominant type of chlorite. The chemical composition of chlorites is governed by dominant $FeMg_{-1}$-substitution and also by Tschermak's substitution and dioctahedral substitution. The content of impurities (K, Ca, Na) is very low. White K-micas were formed mainly by alteration of alkali feldspars or plagioclases and can be divided into: phengitic muscovites and illites. Phengitic muscovites in the phengitic component (Brigatti et al. 2000) range from 0.17 to 0.25. The content of Ti is 0.016–0.020 a.p. 11 oxygens and indicates postmagmatic to hydrothermal origin (Miller et al. 1981). The content of interlayer occupancy (K + Ca + Na) ranges from 0.905 to 0.964 a.p. 11 oxygens and agrees with data from Konings et al. (1984), Piantone et al. (1994) and others. The chemical composition of phengitic muscovites is governed by Tschermak's substitution, dioctahedral-trioctahedral substitution and $A_{-1}(Si_{+1}Al_{-1})^{IV}$-substitution. The phengitic component for illites is 0.02–0.14. The content of Ti (0.005–0.019 a.p. 11 oxygens) indicates hydrothermal origin (Miller et al. 1981). The content of K ranges from 0.770 to 0.926 a.p. 11 oxygens and agrees with data from Cathelineau & Izquierdo (1988), Aja et al. (1991 a,b), Środroń & Eberl (1984) and others. The chemical composition of illites is governed by substitutions $A_{-1}(Si_{+1}Al_{-1})^{IV}$ -substitution, dioctahedral-trioctahedral substitution and Tschermak's substitution.

Key words: Sb-Au deposit, granitoid rocks, illite, phengitic muscovite, magnesium chamosite, ferrous clinochlore, annite, phlogopite.

Introduction

The Pezinok-Kolársky vrch Hill Sb-Au deposit (Malé Karpaty Mts, below only PKV Sb-Au deposit) has been studied quite often in the last decades (Cambel 1959; Chovan et al. 1992 and others). Nonetheless, the study of hydrothermal alteration has been given relatively little attention. Some basic information about hydrothermal alterations and processes connected with alteration were published in Andráš (1983). The present paper presents some results of our study of the chemical composition of phyllosilicates from hydrothermally altered granitoid rocks.

The PKV Sb-Au deposit is situated in the Hrubá dolina Valley on the NE edge of the Pezinské Karpaty Mts (part of the Malé Karpaty Mts) approximately 7 km NNW from Pezinok. From 1790 to 1811, and from 1914 to 1991, it was an important source of Sb. Approximately one million tons of Sb ore has been mined from this deposit.

Methods

The samples of granitoid rocks were collected from the Pyritová adit and New Alexander adit. They represent less (A.I. < 0.35), more (A.I. = 0.35–0.50) and strongly (A.I. > 0.50) altered rocks (see A.I. — alteration index defined by Hashiguchi et al. (in Vivallo 1987) and evaluated as the ratio: $(MgO + K_2O)/(Na_2O + K_2O + CaO + MgO)$ in Table 1).

Polished thin sections of these samples were studied in transmitted light and were then prepared for microprobe analysis. Electron microprobe analyses were performed by JEOL 733 Superprobe (Geological Survey of the Slovak Republic) at 15 kV accelerating voltage, 1.1–1.4 mA sample current and the following standards: Si — SiO_2, Ti — TiO_2, Al — Al_2O_3, Fe — Fe_2O_3, Mn — rodonite, Mg — MgO, Ca — wollastonite, Na — albite, K — orthoclase and Cr — chromite.

Formulae for micas and chlorites were calculated on the basis of 11 oxygen (Bailey 1984; Rieder et al. 1998) and 14 oxygen atoms (Bailey 1988) using the software Minfile (Afifi & Essene 1988). We have applied Mössbauer spectroscopy in the study of samples PYH-15, PYH-9 and PYH-3 for averaging the ratio of Fe^{3+}/Fe^{2+} and the amount of Fe^{3+} (Lipka 1999). Mössbauer spectra were measured at room temperature using conventional Mössbauer spectrometer (Department of Nuclear Physics and Technology of the Slovak University of Technology) with source ^{57}Co in Rh matrix. Spectra were fitted using the NORMOS program. The accuracy of the IS and QS data is 0.04 mm/s and the accuracy of the relative area is 0.4 %.

X-ray diffraction analyses of clay material were performed on a Phillips PW 1710 diffractometer (Geological Institute of the Slovak Academy of Sciences). Oriented samples were prepared by sedimentation of clay suspension (10 mg/cm^2) on glass plates. They

*Corresponding author: dmoravan@nic.fns.uniba.sk

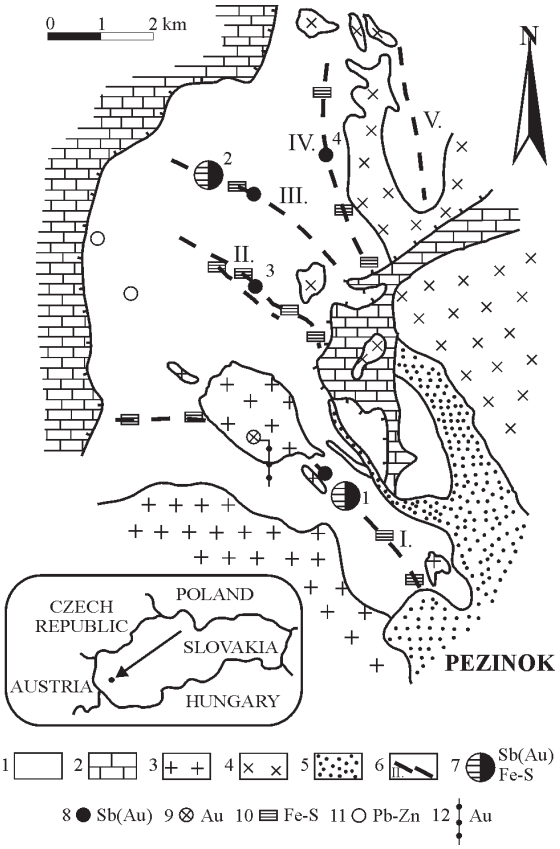

Fig. 1. Schematic geological map of the Pezinok-Pernek deposit crystalline complex with marked deposits and occurrences of raw materials (Chovan et al. 1992). Legend: **1** — metamorphic rocks of the central deposit area, **2** — Mesozoic, **3** — granites of the Bratislava Massif, **4** — granodiorites of the Modra Massif, **5** — Quarternary, **6** — productive zones with black schists and stibnite–gold and pyrite mineralization, **7** — deposits of Sb, Au, and Fe ores (1 — Pezinok-Kolársky vrch Hill, 2 — Pernek), **8** — occurrences of Sb, Au ores (3 — Trojárová, 4 — Kuchyňa), **9** — gold occurrence (Staré Mesto), **10** — occurrences of pyrite ores, **11** — occurrences of polymetallic and copper ores, **12** — gold placers. Inset shows localization of the Pezinok Sb-Au deposit in Slovakia.

were analyzed in the range 2°–50° 2Θ, with CuKα radiation, Ni filter, 35 kV generator voltage, 20 mA tube current and divergence slit, fixed, 1.0 and receiving slit 0.2. The scan step size was 0.02° and scan step time was 0.8 s.

Bulk rock chemistry was determined by wet chemical analysis (major oxides) and combination of AAS and ICP (trace elements, Geological Survey of the Slovak Republic).

Geological setting and petrology

The Pezinok-Kolársky vrch Hill Sb-Au deposit (Fig. 1) lies among crystalline schists (amphiboles, actinolite schists, gneisses, phyllites) intersected by vein bodies of Variscan granitoids. The Sb-Au mineralization is associated with a large fault zone and petrographically variable black schists and phyllites.

Mineral parageneses have been studied by Cambel (1959). On the basis of Cambel's results as well as his own studies, Andráš (1983) distinguished four mineralization stages during which the hydrothermal Sb-Au mineralization formed: stage 1: quartz–arsenopyrite, with gold associated with arsenopyrite and pyrite, stage 2: quartz–pyrite–arsenopyrite ± löllingite, tetrahedrite, chalcopyrite, stage 3: quartz–carbonate–stibnite ± gudmundite, pyrrhotite, pyrite, sphalerite, Pb–Sb sulphosalts, berthierite, stage 4: stibnite–kermesite ± antimony, valentinite, schafarzikite. The principal ore mineral of Sb-mineralization is stibnite, in some zones there is an increased content of berthierite, or sometimes gudmundite and primary kermesite (Chovan et al. 1992).

Granitoid rocks associated with PKV Sb-Au deposit are represented by the peraluminous two-mica granites to granodiorites of the Bratislava granitoid massif. These rocks are enriched in quartz, contain monazite (± ilmenite) and they are characterized as S-type (Cambel & Petrík 1982; Petrík et al. 1994). The rock-forming mineral assemblage of unaltered rocks comprises Fe-biotite, primary muscovite, plagioclase, sericitized K-feldspar and quartz. Plagioclases (17–28 vol. %) are represented by oligoclase with An_{16-25}, in leucocratic type with An_{12-15}. They are slightly saussuritized and are zoned with basic cores and acidic rims. Perthitic K-feldspars (18–33 vol. %) are represented by microcline or orthoclase in varying amounts. K-feldspars are only very slightly sericitized. Quartz is abundant (27–28 vol. %). Biotite (4–16 vol. %, with $Fe_{tot}/(Fe_{tot} + Mg) = 0.64–0.68$) is more abundant than muscovite (6 vol. %). Biotites often show incipient chloritization, epidotization, or are altered to muscovites. The chemical composition of primary celadonitic muscovites ($Al^{IV}/(Al^{IV} + Si) = 0.17–0.24$ and $TiO_2 = 0.48–0.97$ wt. %) is close to phengites (Cambel & Vilinovič 1987; Petrík 1985).

Geochronological data from granitoid rocks of the Malé Karpaty Mts yield the age 347 ± 4 Ma (Rb-Sr isochrone method) and $(^{87}Sr/^{86}Sr)_0 = 0.7076 \pm 0.0013$ for granitoids of the Bratislava Massif.

Results

Granitoid rocks from the PKV Sb-Au deposit can be divided according to alteration index (Hashiguchi et al. in Vivallo 1987) into three groups: less altered rocks (Pyritová adit, PYH-15, A.I. = 0.33), more altered rocks (PYH-9, A.I. = 0.38, PYH-3, A.I. = 0.41) and strongly altered rocks (New Alexander adit, NAŠH-19, A.I. = 0.56, NAŠH-20, A.I. = 0.59).

The rock-forming mineral assemblage in less and more altered rocks comprises plagioclase (andesine, oligoclase to albite), Mg- to Fe-biotite and quartz. K-feldspars are probably albitized or completely altered to white K-micas. Mg- to Fe-biotites are gradually altered to chlorites. Rutile or sphene are a by-product of this alteration. Plagioclases are altered to white K-micas and carbonates. White K-micas intergrow with fine-grained carbonates and they are dominant in more altered rocks with A.I. = 0.41. Remnants of allotriomorphic grains of feldspar and quartz are preserved locally.

The original rock-forming mineral assemblage in the strongly altered rocks (A.I. = 0.56–0.59) could not be identified. Apart from newly-formed micas and fine-grained carbonates, the rocks also contain allotriomorphic remnants of quartz, ± feldspar and primary/postmagmatic muscovite.

The chemical composition of altered granitoid rocks is given in Table 1. Analyses of less altered rock (PYH-15) and more altered rock (PYH-9) in the multicationic diagram $Q_3B_3F_3$ (de la Roche 1980) lie near average granodiorite (see Fig. 2) and this finding agrees with the results of Cambel & Petrík (1982). Strongly altered rocks show that SiO_2, Na_2O were removed and Al_2O_3, Fe_2O_3, TiO_2, CaO, MgO, K_2O and CO_2 were added to the rocks during hydrothermal alteration. The bulk rock chemistry and the rock-forming mineral assemblage of strongly altered samples (NAŠH-19, NAŠH-20) indicate different magmatic precursor as metaaluminous to aluminous granodiorites of Modra granitoid massif. We suppose that

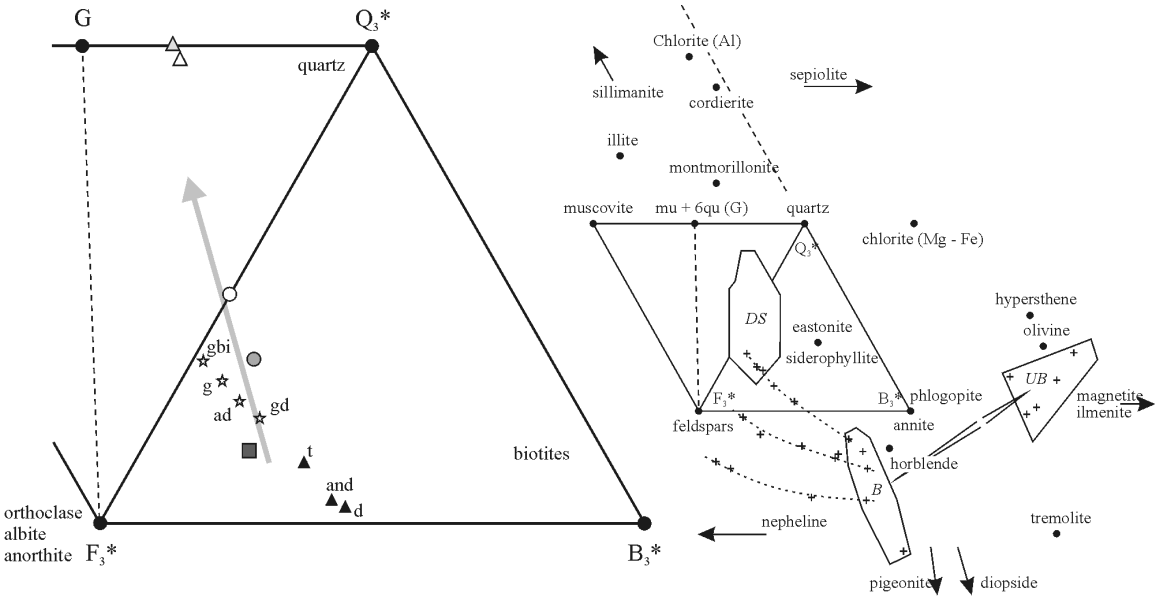

$Q_3 = Si + 7.Al/2 - 9.Ca - 13.(Na + K)/2$
$B_3 = -7.Al/2 + 7.Ca + 7.(Na + K)/2 + 8.(Mg + Fe + Ti)/3$
$F_3 = + Al + 3.Ca + 4.(Na + K) - 5.(Mg + Fe + Ti)/3$
$\Sigma = Si + Ca + (Na + K) + (Mg + Fe + Ti)$

Legend: ■ less altered rock (PYH-15, A.I. = 0.33), ● more altered rock (PYH-9, A.I. = 0.38), ○ more altered rock (PYH-3, A.I. = 0.41), △ strongly altered rock (NAŠH-19, A.I. = 0.57), ▲ strongly altered rock (NAŠH-20, A.I. = 0.60).

Fig. 2. The quartz-muscovite-feldspars-biotite rhombus, extension of the $Q_3B_3F_3$ triangle (de la Roche 1980). Rocks and minerals: **g** — granites, **gbi** — biotite granites, **ad** — adamellites, **gd** — granodiorites, **t** — tonalites, **d** — diorites, **and** — andesites, **B** — basic rocks, **UB** — ultrabasic rocks, **DS** — detritic sedimentation, **qu** — quartz, **mu** — muscovite. The grey arrow shows increasing degree of hydrothermal alteration.

precursor of sample NAŠH-19 and NAŠH-20 was peraluminous two-mica granite of the Bratislava granitoid massif.

Chemical composition of biotites

Biotites from less altered rocks (see Fig. 10A) have a higher content of Mg (1.386–1.580 atoms per 11 oxygens), a lower content of Fe_{tot} (1.266–1.232 a.p. 11 oxygens), ratio $Fe_{tot}/(Fe_{tot} + Mg)$ = 0.43–0.48 and the content of Ti is 0.136–0.223 a.p. 11 oxygens. The amount of Fe^{3+} in the biotite sample PYH-15 is 7.9 %. The ferrous doublets QS_1 and QS_2 should be attributed to iron in ideal M1 and M2 sites. For the good fit in the spectrum for sample PYH-15 it was necessary to add one more doublet QS_3 with the relative area of about 2.1 %. The QS and IS parameters of this doublet are between those which are usually observed for Fe^{2+} and Fe^{3+}. Corresponding Mössbauer spectrum is given in Fig. 5A and the quantitative data are summarized in Table 6. The main type of substitution appears to be combined Al- and Ti-Tschermak's substitution (Fig. 3A,B). Al-Tschermak's substitution according to the reaction:

$$(R^{2+})^{VI} + (Si^{4+})^{IV} = (Al^{3+})^{VI} + (Al^{3+})^{IV} \quad (1),$$

is the dominant mechanism of Al-substitution in biotites. The effect of this substitution is maximized if biotites are found to coexist with Al-saturated phases (Tracy & Robinson 1978) and the final result of this substitution is the end-member eastonite $KMg_2AlAl_2Si_2O_{10}(OH)_2$.

The Al content in biotites from rocks of the PKV Sb-Au deposit ranges from 1.373 to 1.559 a.p. 11 oxygens. If we suppose, that the content of Si ranges from 2.606 to 2.655 a.p. 11 oxygens, then redundant Al ($\sum$T site = 4) has to be associated with an octahedral site. Attendance of Al in octahedral site

Table 1: Bulk chemical composition of altered granitoid rocks from the Pezinok Sb-Au deposit. Oxides in wt. %, trace elements in ppm, Au in g/t, and A.I. = alteration index (see text). Analyses of altered granitoids are arranged in the order of increasing A.I. **L.A.** — less altered rocks, **M.A.** — more altered rocks, **S.A.** — strongly altered rocks.

	SAMPLE				
	PYH-15 (L.A.)	**PYH-9 (M.A.)**	**PYH-3 (M.A.)**	**NAŠH-19 (S.A.)**	**NAŠH-20 (S.A.)**
SiO_2	63.83	55.86	47.94	63.05	61.15
Al_2O_3	15.93	17.99	18.34	15.39	15.76
Fe_2O_3	4.50	7.30	5.15	3.60	3.78
TiO_2	0.759	1.293	1.52	0.649	0.651
CaO	3.97	4.26	6.93	4.22	4.20
MgO	1.63	2.89	3.78	1.64	1.89
MnO	0.067	0.059	0.144	0.100	0.124
P_2O_5	0.26	0.41	0.35	0.24	0.23
Na_2O	4.54	4.05	3.23	0.12	0.13
K_2O	2.64	2.13	3.41	4.09	4.38
S_{tot}	0.18	0.14	<0.01	0.86	1.02
SO_3	<0.01	<0.01	<0.01	0.02	0.01
H_2O^+	0.41	0.48	0.43	0.31	0.29
H_2O^-	0.31	0.28	0.35	0.28	0.32
CO_2	0.04	1.00	6.98	4.64	4.77
Total	99.076	98.152	98.574	99.209	98.705
Rb	72	65	124	181	199
Ba	1331	1378	709	613	687
Sr	804	801	181	101	111
V	76	114	204	130	73
Cr	20	19	58	22	16
Ni	33	7	19	9	5
Cu	10	11	3	14	15
Y	12	13	17	20	17
Zr	264	393	224	246	242
Nb	10	10	12	10	9
Hf	6	9	6	6	6
As	13	2	43	4323	1627
Sb	68	17	26	174	69
Au	<0.005	<0.005	<0.005	1.90	0.74
Hg	0.01	0.01	<0.01	0.01	0.01
Th	5	6	9	7	7
U	<5	<5	<5	<5	<5
Co	9	11	16	5	5
B	11	25	151	163	172
Mo	0.9	1.2	0.4	1.6	1.9
A.I.	0.33	0.38	0.41	0.57	0.60

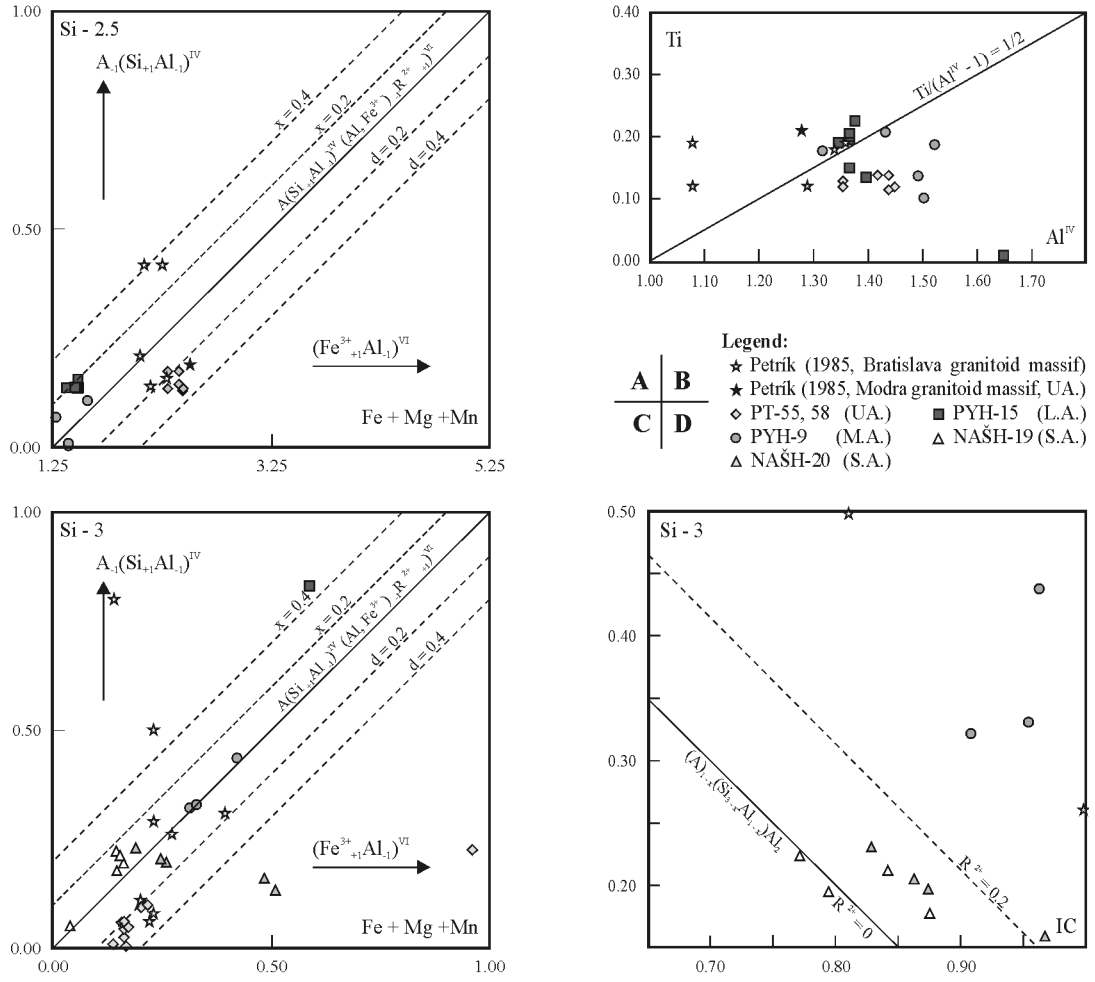

Fig. 3. Substitutions in biotites, phengitic muscovites and illites from the Pezinok Sb-Au deposit. **A** — (Si – 2.5) – (Fe + Mg + Mn) plot of biotites, x = Si – 2.5, d = Fe + Mg + Mn, A = K + Ca + Na. **B** — Ti – and Al^{IV}– contents of biotites. **C** — (Si – 3) – (Fe + Mg + Mn) plot of phengitic muscovites and illites, x = Si – 3, d = Fe + Mg + Mn, A = K + Ca + Na. **D** — (Si – 3) – IC (interlayer charge) plot of phengitic muscovites and illites, the unbroken line gives the theoretical trend corresponding to the $(A_{-1}(Si_{+1}Al_{-1}))$ substitution, A = K + Ca + Na.

cannot be interpreted by substitution (1). Foster (1960a,b) suggested that the additional Al is incorporated into biotite by means of a dioctahedral-trioctahedral substitution:

$$3(R^{2+})^{VI} = 2(Al^{3+})^{VI} + \square^{VI} \quad (2),$$

which could be viewed as a muscovite component in biotite and results in the formation of octahedral vacancies ($\square^{VI}$). The low content of octahedral Al^{VI} in biotites from the PKV Sb-Au deposit (0.077–0.165 a.p. 11 oxygens) indicates complementary character of substitution (2) to substitution (1).

Ti-substitution in biotite is a problematic type of substitution. While, Engel & Engel (1960) suggested that Ti^{3+} replaces Al^{3+} on an octahedral site, many other authors have suggested the attendance of Ti^{4+} (Aubrecht & Hewitt 1980; Dymek 1983; Hewitt & Aubrecht 1986 and others). Ti^{4+}-substitution in an octahedral site is complicated by its high charge and small cation radius (0.605×10^{-1} nm) compared to Mg^{2+} (0.72×10^{-1} nm) and Fe^{2+} (0.78×10^{-1} nm) (ionic radii from Shannon & Prewitt 1969).

Several substitution mechanisms have been suggested for interpretation of this type of substitution. The first involves a coupled substitution for an octahedral and tetrahedral site according to the reaction:

$$(R^{2+})^{VI} + 2(Si^{4+})^{IV} = (Ti^{4+})^{VI} + 2(Al^{3+})^{IV} \quad (3).$$

Substitution (3) can be viewed as a Ti-Tschermak's component (see Fig. 3A,B) leading to the theoretical end-member Ti-eastonite $KMg_2TiSiAl_3O_{10}(OH)_2$ (Czamanske & Wones 1973). A second coupled substitution would be according to the reaction:

$$(Al^{3+})^{VI} + (Si^{4+})^{IV} = (Ti^{4+})^{VI} + (Al^{3+})^{IV} \quad (4).$$

Direct substitution of Ti for Al on octahedral site according to Forbes & Flower (1974), Dymek & Albee (1977) and also substitution according to the dehydrogenation reaction:

$$(R^{2+})^{VI} + 2(OH)^{-} = (Ti^{4+})^{VI} + 2(O^{2+}) + H_2 \quad (5),$$

are probably not for biotites from the PKV Sb-Au deposit. This type of substitution leads to the theoretical end-member Ti-oxybiotite $KMg_2TiSi_3AlO_{12}$.

The range of Fe^{3+}-Tschermak's substitution appears to be very small. An additional important mechanism relevant to Fe^{3+} in biotite involved in situ oxidation Fe^{2+}, is represented by the following reaction:

$$Fe^{2+} + (OH)^{-} = Fe^{3+} + O^{2+} + 1/2\ H_2 \quad (6).$$

Many aspects of the resulting oxyannite end-member $KFe^{2+}Fe^{3+}Si_3AlO_{12}$ were discussed by Eugster & Wones (1962), Wones (1963a,b) and Wones & Eugster (1965). In the

examined rocks from PKV Sb-Au deposit we consider that substitution (6) could be more important than Fe^{3+}-Tschermak's substitution.

Substitutions (1), (2), (3), and possibly also substitution (4), are combined with interlayer deficient occupancy on the A site. Chemical variation on the A site in biotite may arise from at least two sources. Substitution H_3O^+ for K^+ could explain a low concentration of interlayer cations. This type of substitution in biotites from the PKV Sb-Au deposit could not be confirmed.

We consider that interlayer deficient occupancy on the A site (0.826–0.942 a.p. 11 oxygens) can be explained according to the reaction:

$$(K^+)^A + (Al^{3+})^{IV} = \square^A + (Si^{4+})^{IV} \quad (7),$$

which relates phlogopite–annite to a talc component $\square^A(MgFe^{2+})_3Si_4O_{10}(OH)_2$ (Dymek 1983; Hewitt & Aubrecht 1986). Average formula of biotites from PKV Sb-Au deposit is: $(K_{0.910})(Mg_{1.477}Fe^{2+}_{1.143}Fe^{3+}_{0.108}Mn_{0.011}Ti_{0.188}Al_{0.104})(Si_{2.633}Al_{1.367})O_{10}(OH)_2$.

Biotites from more altered rocks (see Fig. 10B) have a higher content of Fe_{tot} (1.461–1.749 a.p. 11 oxygens) and lower content of Mg (1.185–1.464 a.p. 11 oxygens). The ratio $Fe_{tot}/(Fe_{tot} + Mg)$ = 0.53–0.55 and the content of Ti is 0.107–0.211 a.p. 11 oxygens. The relative amount of Fe^{3+} in the biotite sample PYH-9 is only 2.2 %. The ferrous doublets QS_1 and QS_2 should be attributed to iron in ideal M1 and M2 sites. Corresponding Mössbauer spectrum is given in Fig. 5B and the quantitative data are summarized in Table 6. Substitutions in these biotites are similar to substitutions in biotites from less altered rocks. Whereas the greater portion of analyses in the Ti-Al^{IV} diagram lie below the Ti/(Al^{IV}–1) = 1/2 line (Fig. 3B), we consider that Al-Tschermak's substitution according to reaction (1) is the dominant type of substitution. Interlayer deficient occupancy is higher than in the previous case (0.595–0.771 vs. 0.826–0.942 a.p. 11 oxygens) and indicates the presence of substitution (7). The average formula is: $(K_{0.512})(Mg_{1.346}Fe^{2+}_{1.559}Fe^{3+}_{0.035}Mn_{0.015}Ti_{0.166}Al_{0.119})(Si_{2.549}Al_{1.451})O_{10}(OH)_2$.

Biotites from unaltered/less altered granitoid rocks (Petrík 1985, ZK-50, ZK-51, ZK-53, ZK-60, ZK-126 (Bratislava granitoid massif) and ZK-5 (Modra granitoid massif)) have a higher content of Fe_{tot} (1.186–1.572 a.p. 11 oxygens) and Mg (0.684–1.331 a.p. 11 oxygens). The ratio $Fe_{tot}/(Fe_{tot} + Mg)$ = 0.47–0.68 and content of Ti is 0.119–0.209 a.p. 11 oxygens. Our study of granitoid rocks from borehole PT-58 (locality Trojárová) yielded similar conclusions. These samples have a higher content of Fe_{tot} (1.494–1.674 a.p. 11 oxygens) and Mg (0.746–0.848 a.p. 11 oxygens). The ratio $Fe_{tot}/(Fe_{tot} + Mg)$ = 0.65–0.83 and content of Ti is 0.080–0.146 a.p. 11 oxygens. These conclusions are not in compliance with our results from altered granitoid rocks from Pezinok-Kolársky vrch.

The chemical composition of biotites with regard to end-member phlogopite, annite, eastonite and siderophyllite is shown in Fig. 4 (de Albuquerque 1973). Whereas biotites from less altered rocks can be classified as phlogophites ($Phl_{30.09-45.79}Ann_{26.67-36.00}Eas_{22.93-10.22}Sid_{20.31-8.02}$), biotites from more altered rocks have more Fe than Mg and can be classified as annites ($Phl_{34.79-41.13}Ann_{39.20-46.39}Eas_{12.22-5.86}Sid_{13.79-6.62}$). The ratio of $Fe_{tot}/(Fe_{tot} + Mg)$, the rock-forming mineral assemblage and the multicationic $Q_3B_3F_3$ (de la Roche 1980) indi-

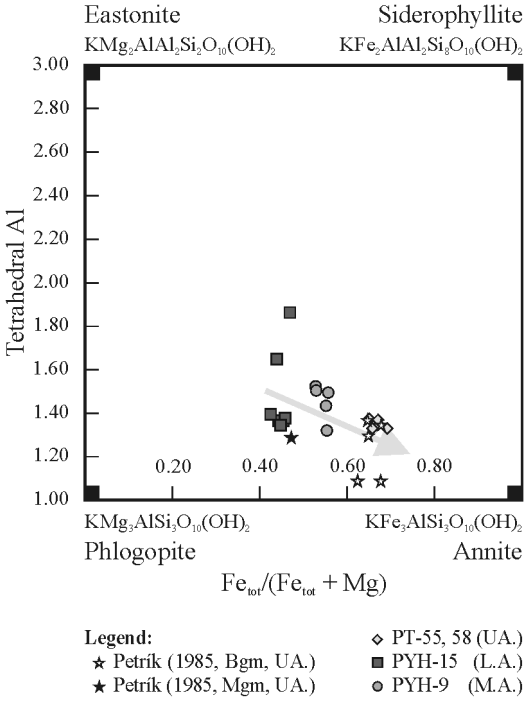

Fig. 4. Chemical composition of biotites from the Pezinok Sb-Au deposit with regard to end-members phlogopite, annite, eastonite and siderophyllite (de Albuquerque 1973). The grey arrow shows increasing degree of hydrothermal alteration.

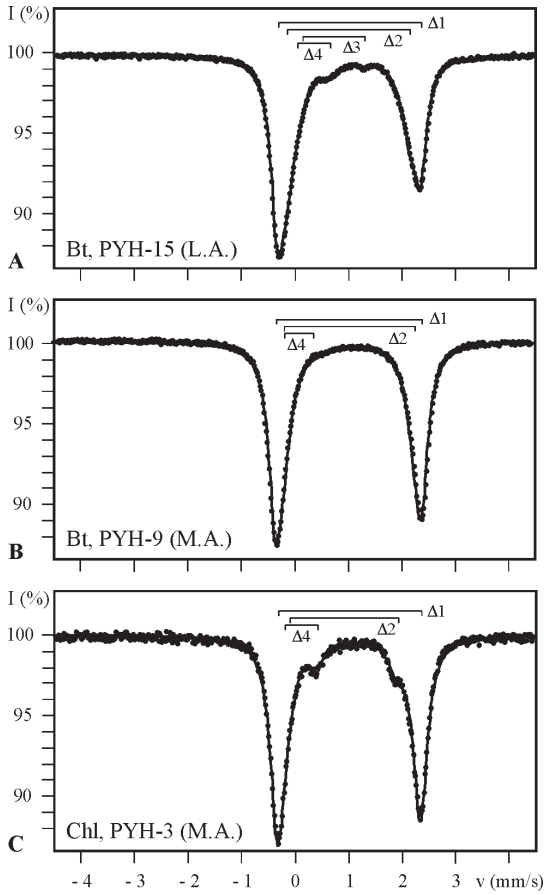

Fig. 5. Room temperature Mössbauer spectra of studied samples from the Pezinok Sb-Au deposit. **A** — biotite sample PYH-15, **B** — biotite sample PYH-9 and **C** — chlorite sample PYH-3.

cates that the studied granitoid rocks are close to metaaluminous to peraluminous granodiorites of Modra granitoid massif. Granodiorites from the Modra granitoid massif are enriched in plagioclase, contain amphibole, accessory epidote, titanite, allanite and they are characterized as I-type (Cambel & Petrík 1982; Petrík et al. 1994). Selected electron microprobe analyses of biotite and biotite-like material, the ratio in percent of single components and ratio $Fe_{tot}/(Fe_{tot} + Mg)$ are given in Table 3 and Table 5.

Chemical composition of chlorites

Chlorite-like material from less altered rocks (see Fig. 10A) differs from the theoretically possible chemical composition of chlorites according to Wiewióra & Weiss (1990) or Weiss (1991). It is caused by incomplete alteration of biotites into chlorites (ΣR = 6.114–6.258 a.p.f.u.). Because these "chlorites" do not have octahedral vacancies, we can eliminate the presence of dioctahedral substitution (according to the reaction 2). The Fe_{tot} content ranges from 1.920 to 2.458 a.p.f.u., the Mg content ranges from 2.639 to 3.099 a.p.f.u. and the ratio $Fe_{tot}/(Fe_{tot} + Mg)$ is 0.53–0.62. We suppose that the relative amount of Fe^{3+} in chlorite sample PYH-15 is similar to the relative amount of Fe^{3+} in biotite sample PYH-15. The average formula is: $(Mg_{2.886}Fe^{2+}_{2.092}Fe^{3+}_{0.197}Mn_{0.028}Al_{0.971}Ti_{0.038})(Si_{2.664}Al_{1.336})O_{10}(OH)_8$ and this formula corresponds to ferrous clinochlore. Magnesium chamosites have not been identified in less altered rocks. $FeMg_{-1}$-substitution and Tschermak's substitution (according to the reaction 1 and 3) are present only over a small range. Octahedral Al ranges from 0.933 to 1.008 a.p.f.u.

Identified tri-trioctahedral chlorites (ΣR = 5.510–5.917, $\square^{VI}$ = 0.090–0.483 a.p.f.u.) belong to clinochlore-chamosite series and originated from biotites. According to the Wiewióra & Weiss (1990) or Weiss (1991) classification they can be divided into two groups: ferrous clinochlores (schematic formula $Mg_{34.39-36.32}Fe_{28.31-37.07}X_{24.02-35.39}$) and magnesium chamosites (schematic formula $Mg_{34.33-37.90}Fe_{34.76-39.32}X_{23.18-28.30}$, see Fig. 6).

Chlorites from more altered rocks, with A.I. = 0.38–0.41 (see Fig. 10D), range in the Fe_{tot} from 1.561 to 2.301 a.p.f.u, whilst the content of Mg ranges from 1.929 to 2.291 a.p.f.u.. The ratio $Fe_{tot}/(Fe_{tot} + Mg)$ = 0.48–0.56. We suppose that the relative amount of Fe^{3+} in chlorite sample PYH-9 is similar to the relative amount of Fe^{3+} in biotite sample PYH-9. The relative amount of Fe^{3+} of chlorite sample PYH-3 is 9.3 %, the rest of the iron is in two-valence state. Mössbauer spectrum was fitted with two doublets (QS_1 and QS_2), which correspond to Fe^{2+}, and with doublet QS_4 that corresponds to Fe^{3+}. Corresponding Mössbauer spectrum is given in Fig. 5C and the quantitative data are summarized in Table 6. The contents of impurities are very low (Ca = 0.007–0.047, K = 0.035–0.278 a.p.f.u.). The average formula is: $(Mg_{2.160}Fe^{2+}_{1.831}Fe^{3+}_{0.139}Mn_{0.005}Al_{1.381}Ti_{0.098}\square_{0.386})(Si_{2.965}Al_{1.035})O_{10}(OH)_8$, for ferrous clinochlores and $(Mg_{2.083}Fe^{2+}_{1.991}Fe^{3+}_{0.205}Mn_{0.006}Al_{1.406}Ti_{0.042}\square_{0.267})(Si_{2.944}Al_{1.056})O_{10}(OH)_8$, for magnesium chamosites.

The presence of ferrous clinochlores and the presence of magnesium chamosites in our samples indicates dominant $FeMg_{-1}$-substitution. The ratio Fe_{tot} : Mg in more altered rocks

Table 2: The d spacing data (in nm × 10) and intensites from XRD patterns of clay material from altered granitoid rocks of the Pezinok Sb-Au deposit. Ref. sample: **Chl_K** — clinochlore, **JCPDS table 19** — 749, **Ill_{1M}** — illite, **JCPDS table 2** — 0462 and **Ill_{2M1}** — illite, **JCPDS table 9** — 334. **Chl** — chlorite, **Ill** — illite, **Qtz** — quartz, **Pl** — plagioclase. **L.A.** — less altered rocks, **M.A.** — more altered rocks, **S.A.** — strongly altered rocks.

REF. SAMPLE						OBS. SAMPLE									
$Chl_{(K)}$		Ill_{1M}		Ill_{2M1}		PYH–15 (L.A.)		PYH–9 (M.A.)		PYH–3 (M.A.)		NAŠH–19 (S.A.)		NAŠH–20 (S.A.)	
$d_{(tab.)}$	$I_{(tab.)}$	$d_{(tab.)}$	$I_{(tab.)}$	$d_{(tab.)}$	$I_{(tab.)}$	$d_{(obs.)}$	$I_{(obs.)}$	$d_{(obs.)}$	$I_{(obs.)}$	$d_{(obs.)}$	$I_{(obs.)}$	$d_{(obs.)}$	$I_{(obs.)}$	$d_{(obs.)}$	$I_{(obs.)}$
14.300	70	-	-	-	-	14.239	36 (Chl)	14.283	42 (Chl)	14.259	31 (Chl)	13.484	3 (Chl)	14.254	1 (Chl)
-	-	10.000	80	-	-	10.049	96 (Ill)	10.025	100 (Ill)	10.055	100 (Ill)	10.078	100 (Ill)	10.098	100 (Ill)
-	-	-	-	9.900	80	-	-	-	-	-	-	-	-	-	-
7.120	100	-	-	-	-	7.096	66 (Chl)	7.109	98 (Chl)	7.095	78 (Chl)	7.068	2 (Chl)	7.111	2 (Chl)
-	-	-	-	-	-	6.375	14 (Pl)	6.392	13 (Pl)	-	-	-	-	-	-
-	-	5.030	80	-	-	-	-	-	-	5.004	30 (Ill)	5.015	30 (Ill)	5.019	30 (Ill)
-	-	-	-	4.900	60	4.999	28 (Ill)	4.990	29 (Ill)	-	-	-	-	-	-
-	-	-	-	-	-	4.723	19 (Chl)	4.728	21 (Chl)	4.723	17 (Chl)	-	-	-	-
4.630	70	-	-	-	-	-	-	-	-	-	-	-	-	-	-
-	-	4.520	60	-	-	-	-	4.535	10 (Ill?)	-		-	-	-	-
-	-	-	-	4.460	100	-	-	-	-	-	-	4.498	2 (Ill)	4.489	2 (Ill)
-	-	-	-	4.290	40	4.250	15 (Qtz)	-	-	-	-	4.258	2 (Qtz)	4.253	1 (Qtz)
-	-	-	-	4.110	40	-	-	-	-	-	-	4.102	2 (Pl)	-	-
-	-	-	-	-	-	4.038	24 (Pl)	4.035	18 (Pl)	-	-	-	-	4.008	1 (Pl)
-	-	-	-	3.880	60	3.879	10 (Pl)	-	-	-	-	-	-	-	-
-	-	-	-	-	-	3.771	18 (Pl)	3.770	11 (Pl)	3.770	5 (Pl)	-	-	-	-
-	-	3.630	80	3.650	50	3.665	15 (Pl)	3.668	12 (Ill)	3.660	5 (Pl)	3.654	2 (Ill)	3.671	2 (Ill)
3.560	80	-	-	-	-	3.540	24 (Chl)	3.543	39 (Chl)	3.538	35 (Chl)	3.537	2 (Chl)	-	-
-	-	3.350	100	3.360	100	3.342	74 (Ill)	3.322	60 (Ill)	3.333	50 (Ill)	3.338	47 (Ill)	3.340	46 (Ill)
-	-	-	-	-	-	3.239	34 (Pl)	-	-	3.193	10 (Pl)	-	-	-	-
-	-	3.100	80	3.100	50	3.190	100 (Pl)	3.192	57 (Pl)	-	-	-	-	-	-
-	-	2.900	80	-	-	2.936	12 (Pl)	-	-	-	-	-	-	-	-
-	-	-	-	2.860	60	-	-	-	-	-	-	-	-	-	-
2.834	40	-	-	-	-	2.836	12 (Chl)	-	-	2.829	9 (Chl)	2.792	2 (Chl)	-	-
2.648	10	-	-	-	-	-	-	-	-	-	-	-	-	2.685	1 (Chl)
-	-	2.600	100	-	-	-	-	-	-	-	-	-	-	-	-
-	-	-	-	2.570	100	-	-	-	-	-	-	-	-	-	-
2.548	80	-	-	-	-	2.552	12 (Chl)	2.562	9 (Chl)	-	-	-	-	2.561	2 (Chl)
-	-	2.470	60	-	-	-	-	2.491	10 (Ill)	2.498	7 (Ill)	2.504	5 (Ill)	2.505	4 (Chl)
2.435	70	-	-	2.450	50	-	-	-	-	-	-	-	-	-	-
2.379	50	2.390	80	2.390	60	2.390	11 (Chl)	-	-	-	-	-	-	-	-
-	-	2.270	40	-	-	2.277	12 (Ill)	-	-	-	-	-	-	-	-
2.255	50	-	-	-	-	-	-	-	-	-	-	-	-	-	-
-	-	-	-	2.240	50	-	-	-	-	-	-	-	-	-	-
-	-	2.180	40	-	-	-	-	-	-	-	-	-	-	-	-
-	-	2.140	80	2.140	60	-	-	-	-	-	-	-	-	-	-
2.000	70	-	-	-	-	-	-	-	-	-	-	2.002	16 (Ill)	2.003	15 (Ill)
-	-	1.990	100	1.992	60	1.988	17 (Ill)	1.989	22 (Ill)	1.997	19 (Ill)	-	-	-	-
-	-	-	-	1.940	40	-	-	-	-	-	-	-	-	-	-

Table 3: Selected electron microprobe analyses of mica and mica-like material from the Pezinok Sb-Au deposit. Oxides in wt. %, analyses are recalculated on the basis of 11 oxygen atoms. **Phl** — phlogopite, **Ann** — annite, **Eas** — eastonite, **Sid** — siderophyllite, **Fe/(Fe + Mg)*** — Fe as Fe_{tot}, **Ph** — phengitic component (see text), **Fe_2O_3*** — calculated on the basis of data from Mössbauer spectroscopy. **L.A.** — less altered rocks, **M.A.** — more altered rocks.

	SAMPLE															
	PYH–15 (L.A.)										PYH–9 (M.A.)					
Mineral	Bt	Bt	Bt	Bt	Bt-Chl	Ms?	Bt	Bt	Bt	Bt	Bt	Bt	Ms_{Ph}	Ms_{Ph}	Ms_{Ph}	Bt
Grain	1	1	1	1	2	2	2	2	2	3	1	1	2	3	3	4
Point	A1	A2	A3	A4	A5	A9	A10	A11	A12	A28	A10	A11	A19	A23	A24	A25
SiO_2	34.61	34.56	34.67	34.94	28.63	57.61	34.55	34.66	34.77	34.59	31.11	29.94	50.51	52.53	50.87	30.85
TiO_2	3.59	3.47	3.91	3.32	1.27	0.86	3.54	3.39	2.63	2.39	3.39	3.03	0.37	0.32	0.40	1.75
Al_2O_3	16.43	16.17	16.08	15.89	17.53	17.73	16.14	16.06	17.09	17.56	15.60	15.91	30.50	27.46	30.12	18.11
Cr_2O_3	0.00	0.00	0.00	0.00	0.00	0.00	0.00	0.00	0.00	0.00	0.00	0.00	0.00	0.00	0.00	0.09
Fe_2O_3*	1.53	1.48	1.54	1.50	1.88	0.00	1.49	1.52	1.49	1.47	0.50	0.52	0.00	0.00	0.00	0.51
FeO	17.78	17.28	17.90	17.52	21.95	4.70	17.33	17.67	17.40	17.19	22.17	22.96	1.88	3.03	1.82	22.57
MnO	0.22	0.16	0.00	0.22	0.24	0.00	0.19	0.27	0.00	0.11	0.24	0.20	0.00	0.00	0.00	0.00
MgO	12.21	13.16	12.78	13.16	17.03	3.30	13.09	12.95	12.94	14.07	10.41	11.85	2.17	2.65	2.38	11.59
CaO	0.33	0.00	0.00	0.00	0.00	0.64	0.00	0.00	0.25	0.00	0.12	0.33	0.22	0.50	0.25	0.10
Na_2O	0.00	0.00	0.00	0.00	0.00	0.00	0.00	0.00	0.69	0.00	0.00	0.00	0.14	1.90	0.69	0.00
K_2O	9.29	9.29	9.72	9.59	3.30	12.66	9.28	9.66	9.74	8.59	5.55	3.56	10.39	8.20	10.11	3.94
Total	95.99	95.54	96.60	96.14	91.83	97.50	95.61	96.18	96.17	96.02	89.09	88.39	96.18	96.59	96.64	89.51
Si^{IV}	2.635	2.635	2.628	2.655	2.286	3.830	2.634	2.638	2.636	2.606	2.568	2.482	3.321	3.436	3.330	2.502
Al^{IV}	1.365	1.365	1.372	1.345	1.649	0.170	1.366	1.362	1.364	1.394	1.432	1.518	0.679	0.564	0.670	1.498
Ti^{IV}	0.000	0.000	0.000	0.000	0.065	0.000	0.000	0.000	0.000	0.000	0.000	0.000	0.000	0.000	0.000	0.000
T site	4.000	4.000	4.000	4.000	4.000	4.000	4.000	4.000	4.000	4.000	4.000	4.000	4.000	4.000	4.000	4.000
Al^{VI}	0.109	0.088	0.064	0.077	0.000	1.219	0.084	0.078	0.163	0.165	0.086	0.036	1.685	1.555	1.654	0.233
Ti^{VI}	0.206	0.199	0.223	0.189	0.012	0.043	0.203	0.194	0.150	0.136	0.211	0.189	0.019	0.016	0.020	0.107
Cr	0.000	0.000	0.000	0.000	0.000	0.000	0.000	0.000	0.000	0.000	0.000	0.000	0.000	0.000	0.000	0.006
Fe^{3+}	0.106	0.103	0.106	0.104	0.137	0.000	0.103	0.105	0.103	0.101	0.034	0.036	0.000	0.000	0.000	0.034
Fe^{2+}	1.124	1.093	1.126	1.105	1.454	0.262	1.097	1.116	1.095	1.075	1.531	1.592	0.104	0.166	0.100	1.531
Mn^{2+}	0.014	0.010	0.000	0.014	0.017	0.000	0.013	0.018	0.007	0.010	0.017	0.014	0.000	0.000	0.000	0.000
Mg	1.386	1.496	1.444	1.491	2.027	0.327	1.488	1.469	1.463	1.580	1.281	1.464	0.213	0.259	0.232	1.401
O site	2.942	2.989	2.963	2.980	3.647	1.851	2.988	3.110	2.981	3.067	3.160	3.331	2.021	1.996	2.006	3.312
Ca	0.027	0.000	0.000	0.000	0.000	0.046	0.000	0.000	0.000	0.000	0.011	0.030	0.016	0.035	0.018	0.009
Na	0.000	0.000	0.000	0.000	0.000	0.000	0.000	0.000	0.000	0.000	0.000	0.000	0.018	0.241	0.088	0.000
K	0.903	0.900	0.940	0.930	0.336	1.074	0.903	0.938	0.942	0.826	0.585	0.386	0.872	0.684	0.845	0.408
A site	0.930	0.900	0.940	0.930	0.336	1.120	0.903	0.938	0.942	0.826	0.596	0.416	0.906	0.960	0.951	0.417
Phl	30.09	45.79	43.90	43.04	-	-	45.79	44.98	44.98	45.77	35.32	34.79	-	-	-	41.13
Ann	26.67	36.00	37.39	35.97	-	-	35.97	36.78	36.78	34.49	43.17	39.20	-	-	-	46.39
Eas	22.93	10.22	10.11	8.98	-	-	10.22	10.04	10.04	11.23	9.69	12.22	-	-	-	5.86
Sid	20.31	8.02	8.60	8.26	-	-	8.02	8.20	8.20	8.51	11.82	13.79	-	-	-	6.62
Fe/(Fe+Mg)*	0.47	0.44	0.46	0.48	-	-	0.44	0.45	0.45	0.43	0.55	0.53	-	-	-	0.53
Ph	-	-	-	-	-	0.34	-	-	-	-	-	-	0.17	0.22	0.17	-

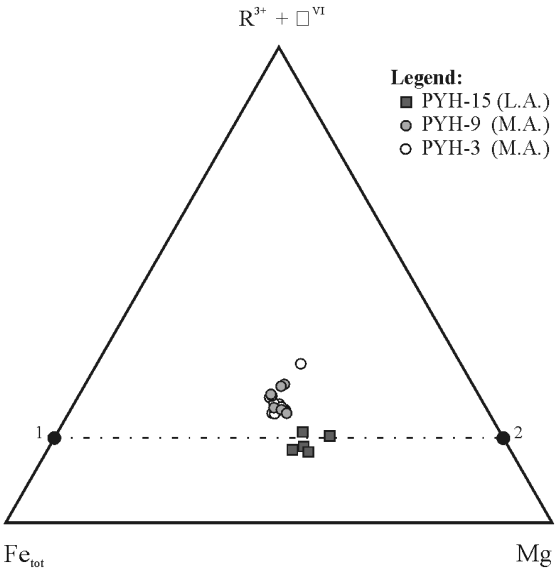

Fig. 6. Triangular diagram Fe_{tot}, Mg and R^{3+} + □ (Weiss 1991) for chlorites from Pezinok Sb-Au deposit. **1** — chamosite, **2** — clinochlore.

is approximately 1 : 1, as shown in Fig. 6. Since these chlorites have ∑R = 5.510–5.917 a.p.f.u. in an octahedral site, we have suggested the present of the dioctahedral substitution (Wiewióra & Weiss 1990; Wiess 1991; Zane & Weiss 1998) according to reaction (2). This type of substitution causes octahedral vacancies ($□^{VI}$ = 0.090–0.483 a.p.f.u.) leading to the formation of tri-dioctahedral chlorites as indicated in some analyses, on Fig. 7.

The Al content in analysed chlorites ranges from 2.162 to 2.750 a.p.f.u. If the content of Si ranges from 2.838 to 3.219 a.p.f.u., then the excess of Al has to be associated with octahedral site (Al^{VI} = 1.229–1.526 a.p.f.u.). The presence of Al on an octahedral site can be explained only with the help of Tschermak's substitution (Foster 1962) according to the reaction (1 and 3) where R^{2+} = Mg, Fe^{2+}, Mn and R^{3+} = Al, Fe^{3+} and Cr. Chemical composition of chlorites according to the Wiewióra & Weiss (1990) or Weiss (1991) classification is shown in Fig. 7. Ferrous clinochlore is the dominant type of chlorite. The present of clinochlore has also been confirmed by X-ray study of clay material (see Table 2). Selected electron microprobe analyses of chlorite and chlorite-like material and the ratio $Fe_{tot}/(Fe_{tot} + Mg)$ are given in Table 4.

Chemical compositions of white K-micas

White K-micas were formed mainly by the alteration of alkali feldspars or plagioclases and can be divided into: phengitic muscovites and illites.

Phengitic muscovites from more altered rocks (see Fig. 10C) have a lower content of Fe_{tot} (0.100–0.161 a.p. 11 oxygens) and Mg (0.213–0.259 a.p. 11 oxygens). The phengitic component (Brigatti et al. 2000) evaluated as a percentage of the ratio $(Fe^{2+} + Fe^{3+} + Mg + Ti + Mn)/(Fe^{2+} + Fe^{3+} + Mg + Ti + Mn + Al)$ is 0.17–0.25. The Ti ranges from 0.016 to

Table 4: Selected electron microprobe analyses of chlorite and chlorite-like material from the Pezinok Sb-Au deposit. Oxides in wt. %, analyses are recalculated on the basis of 14 oxygen atoms. **Fe/(Fe + Mg)*** — Fe as Fe_{tot}, **Fe_2O_3*** — calculated on the basis data from Mössbauer spectroscopy. **L.A.** — less altered rocks, **M.A.** — more altered rocks, **S.A.** — strongly altered rocks.

	SAMPLE															
	PYH–15 (L.A.)			PYH–9 (M.A.)			PYH–3 (M.A.)									
Mineral	Chl	Chl	Chl	Chl	Chl	Chl	Chl	Chl	Chl	Chl	Chl	Chl	Chl	Chl	Chl	Chl
Grain	1	1	1	1	1	2	2	2	3	4	1	1	2	1	1	2
Point	A6	A7	A15	A7	A12	A20	A1	A2	A3	A4	A5	A19	A20	A21	A2	A6
SiO_2	23.61	26.54	24.01	27.28	28.61	30.54	26.28	27.62	27.71	29.45	28.25	25.99	27.97	27.60	27.14	25.88
TiO_2	0.11	1.08	0.00	0.85	4.16	0.80	0.10	0.17	0.60	3.80	0.00	0.00	0.00	0.10	0.00	0.23
Al_2O_3	19.22	18.21	18.27	18.66	17.25	17.82	19.78	19.97	20.08	20.70	19.76	19.96	19.38	19.83	20.61	21.75
Fe_2O_3*	2.04	1.90	2.14	0.53	0.46	0.52	2.39	2.24	2.25	1.69	2.26	2.37	2.24	2.29	2.30	2.30
FeO	23.77	22.10	24.99	23.43	20.30	23.29	23.27	21.89	21.92	16.53	22.09	23.07	21.86	22.30	22.43	22.43
MnO	0.45	0.38	0.37	0.12	0.00	0.26	0.11	0.00	0.00	0.00	0.00	0.00	0.00	0.00	0.00	0.00
MgO	18.24	16.67	17.93	14.33	12.27	12.28	13.70	13.79	12.69	13.09	12.64	13.92	14.61	13.40	14.63	12.93
CaO	0.00	0.10	0.00	0.09	0.23	0.42	0.07	0.00	0.00	0.06	0.00	0.15	0.07	0.00	0.06	0.00
Na_2O	0.00	0.00	0.00	0.00	0.00	0.00	0.00	0.00	0.00	0.00	0.00	0.00	0.00	0.00	0.00	0.00
K_2O	0.17	2.38	0.00	0.64	1.82	0.26	0.00	0.44	0.62	1.03	0.70	0.00	0.28	0.31	0.00	0.46
Total	87.61	89.36	87.17	85.93	85.10	86.19	85.70	86.12	85.87	85.34	85.70	85.46	86.41	85.83	87.17	85.62
Si^{IV}	2.530	2.768	2.601	2.956	3.057	3.219	2.838	2.933	2.954	3.016	3.017	2.811	2.959	2.946	2.851	2.776
Al^{IV}	1.470	1.232	1.399	1.044	0.943	0.781	1.162	1.067	1.056	0.984	0.983	1.189	1.041	1.054	1.149	1.224
T site	4.000	4.000	4.000	4.000	4.000	4.000	4.000	4.000	4.000	4.000	4.000	4.000	4.000	4.000	4.000	4.000
Al^{VI}	0.958	1.007	0.933	1.288	1.229	1.432	1.355	1.433	1.476	1.515	1.504	1.355	1.376	1.441	1.402	1.526
Ti^{VI}	0.009	0.085	0.000	0.068	0.334	0.063	0.008	0.014	0.048	0.293	0.000	0.000	0.000	0.008	0.000	0.019
Fe^{3+}	0.199	0.180	0.211	0.047	0.041	0.046	0.239	0.221	0.222	0.161	0.224	0.237	0.220	0.226	0.224	0.225
Fe^{2+}	2.114	1.914	2.247	2.078	1.814	2.053	2.078	1.922	1.932	1.400	1.951	2.064	1.913	1.969	1.948	1.961
Mn^{2+}	0.041	0.034	0.034	0.011	0.000	0.023	0.010	0.000	0.000	0.000	0.000	0.000	0.000	0.000	0.000	0.000
Mg	2.914	2.639	2.808	2.266	1.954	1.929	2.205	2.183	2.016	1.999	2.012	2.244	2.305	2.132	2.291	2.068
O site	6.258	6.187	6.233	5.855	5.646	5.628	5.895	5.833	5.778	5.510	5.786	5.917	5.850	5.818	5.873	5.862
Ca	0.000	0.011	0.000	0.010	0.026	0.047	0.010	0.000	0.000	0.007	0.000	0.017	0.000	0.000	0.008	0.000
Na	0.000	0.000	0.000	0.000	0.000	0.000	0.000	0.000	0.000	0.000	0.000	0.000	0.000	0.000	0.000	0.000
K	0.023	0.317	0.000	0.087	0.248	0.035	0.000	0.060	0.084	0.135	0.095	0.000	0.038	0.042	0.000	0.063
Fe/(Fe+Mg)*	0.44	0.44	0.47	0.48	0.49	0.52	0.51	0.50	0.52	0.44	0.41	0.37	0.39	0.40	0.49	0.51

Table 5: Selected electron microprobe analyses of mica and mica-like material from the Pezinok Sb-Au deposit. Oxides in wt. %, analyses are recalculated on the basis of 11 oxygen atoms. **Phl** — phlogopite, **Ann** — annite, **Eas** — eastonite, **Sid** — siderophyllite, **Fe/(Fe + Mg)*** — Fe as Fe_{tot}, **Ph** — phengitic component (see text), **Fe_2O_3*** — calculated on the basis of data from Mössbauer spectroscopy. **L.A.** — less altered rocks, **M.A.** — more altered rocks, **S.A.** — strongly altered rocks, **UA.** — unaltered rocks.

	SAMPLE															
	PYH–9 (M.A.)		NAŠH–19 (S.A.)					NAŠH–20 (S.A.)					PT–58 (UA.)			
Mineral	Bt	Bt	Ill	Ill	Ill	Ill	Ill	Ill	Ill	Ill	Ms_{Ph}	Ms_{Ph}	Bt	Bt	Ms	Ms
Grain	4	4	1	2	2	3	5	1	2	2	3	3	1	2	1	2
Point	A26	A27	A1	A2	A3	A4	A5	A33	A34	A35	A38	A39	A25	A31	A6	A9
SiO_2	33.69	29.28	48.45	46.28	49.56	48.98	48.77	47.96	48.79	48.43	46.05	47.06	34.29	33.65	46.49	45.80
TiO_2	3.02	2.17	0.32	0.14	0.18	0.11	0.10	0.38	0.09	0.31	0.33	0.33	2.29	2.06	0.48	0.52
Al_2O_3	15.86	15.40	34.72	37.54	34.79	34.99	34.15	32.83	33.50	33.14	30.85	30.01	18.55	18.40	34.84	35.63
Cr_2O_3	0.00	0.00	0.00	0.00	0.00	0.00	0.15	0.00	0.00	0.00	0.00	0.00	0.00	0.00	0.00	0.00
Fe_2O_3*	0.48	0.54	0.00	0.00	0.00	0.00	0.00	0.00	0.00	0.00	0.00	0.00	0.00	0.00	0.00	0.00
FeO	21.43	23.87	0.78	0.35	0.66	0.73	0.72	1.15	0.77	1.17	1.82	1.56	23.23	25.13	1.73	1.41
MnO	0.00	0.19	0.16	0.00	0.00	0.00	0.00	0.00	0.00	0.00	0.00	0.02	0.57	0.55	0.00	0.00
MgO	9.97	10.96	1.10	0.24	1.16	1.30	1.21	2.00	1.53	1.89	4.02	4.00	6.74	6.88	1.10	0.98
CaO	0.00	0.00	0.00	0.00	0.00	0.00	0.00	0.00	0.00	0.00	0.00	0.00	0.00	0.22	0.00	0.00
Na_2O	0.00	0.00	0.00	0.00	0.00	0.00	0.00	0.00	0.00	0.00	0.00	0.00	0.00	0.00	0.42	0.50
K_2O	7.58	3.80	10.43	11.01	9.27	9.53	10.00	10.25	9.78	10.22	11.01	11.26	9.78	8.88	10.32	11.02
Total	92.03	86.21	95.80	95.60	95.62	95.64	95.10	94.57	94.46	95.14	94.08	95.27	95.45	95.77	95.38	95.86
Si^{IV}	2.686	2.508	3.178	3.052	3.224	3.195	3.212	3.197	3.231	3.205	3.133	3.160	2.675	2.634	3.093	3.043
Al^{IV}	1.314	1.492	0.822	0.948	0.776	0.805	0.788	0.803	0.769	0.795	0.867	0.840	1.325	1.366	0.907	0.957
Ti^{IV}	0.000	0.000	0.000	0.000	0.000	0.000	0.000	0.000	0.000	0.000	0.000	0.000	0.000	0.000	0.000	0.000
T site	4.000	4.000	4.000	4.000	4.000	4.000	4.000	4.000	4.000	4.000	4.000	4.000	4.000	4.000	4.000	4.000
Al^{VI}	0.176	0.064	1.862	1.969	1.892	1.886	1.863	1.776	1.846	1.790	1.607	1.612	0.381	0.331	1.824	1.835
Ti^{VI}	0.181	0.140	0.016	0.007	0.009	0.006	0.005	0.019	0.005	0.016	0.017	0.017	0.135	0.121	0.024	0.026
Cr	0.000	0.000	0.000	0.000	0.000	0.000	0.008	0.000	0.000	0.000	0.000	0.000	0.000	0.000	0.000	0.000
Fe^{3+}	0.032	0.039	0.000	0.000	0.000	0.000	0.000	0.000	0.000	0.000	0.000	0.000	0.000	0.000	0.000	0.000
Fe^{2+}	1.429	1.710	0.043	0.020	0.036	0.040	0.039	0.064	0.043	0.065	0.104	0.087	1.516	1.645	0.096	0.080
Mn^{2+}	0.000	0.014	0.000	0.000	0.000	0.000	0.000	0.000	0.000	0.000	0.000	0.000	0.037	0.036	0.000	0.000
Mg	1.185	1.400	0.108	0.024	0.113	0.126	0.119	0.199	0.151	0.186	0.408	0.400	0.784	0.803	0.109	0.097
O site	3.003	3.367	2.029	2.020	2.050	2.058	2.034	2.058	2.045	2.057	2.136	2.116	3.853	2.133	2.053	2.038
Ca	0.000	0.000	0.000	0.000	0.000	0.000	0.000	0.000	0.000	0.000	0.000	0.000	0.000	0.019	0.000	0.000
Na	0.000	0.000	0.000	0.000	0.000	0.000	0.000	0.000	0.000	0.000	0.000	0.000	0.000	0.000	0.054	0.065
K	0.771	0.416	0.873	0.926	0.770	0.793	0.840	0.872	0.827	0.861	0.956	0.964	0.974	0.887	0.876	0.935
A site	0.771	0.416	0.873	0.926	0.770	0.793	0.840	0.872	0.827	0.861	0.956	0.964	0.974	0.906	0.930	1.000
Phl	37.90	33.97	-	-	-	-	-	-	-	-	-	-	28.48	26.96	-	-
Ann	46.34	41.53	-	-	-	-	-	-	-	-	-	-	55.27	54.74	-	-
Eas	7.09	11.04	-	-	-	-	-	-	-	-	-	-	5.52	6.04	-	-
Sid	8.67	13.46	-	-	-	-	-	-	-	-	-	-	10.73	12.26	-	-
Fe/(Fe+Mg)*	0.55	0.55	-	-	-	-	-	-	-	-	-	-	0.66	0.67	-	-
Ph	-	-	0.08	0.02	0.08	0.08	0.08	0.14	0.14	0.13	0.25	0.24	-	-	0.08	0.07

0.020 a.p. 11 oxygens. This agrees with its hydrothermal origin (see Fig. 8). The dominant relation among the chemical constituents of phengitic muscovites is given by the Tschermak's substitution $(Si_{+1}Al_{-1})^{IV}(Al_{-1}R^{2+}{}_{+1})$ according to reaction (1) and is demonstrated by the strong positive correlation of Si^{IV}/Al^{VI} (Fig. 3C). This substitution is combined with the important dioctahedral-trioctahedral substitution (2, $\square^{VI}$ = 0.864–0.994 a.p. 11 oxygens) and with the low $A_{-1}(Si_{+1}Al_{-1})^{IV}$

Table 6: Parameters (QS, IS) and relative areas (A_{rel}) of the components from biotite samples and chlorite sample of the Pezinok Sb-Au deposit. **L.A.** — less altered rocks, **M.A.** — more altered rocks, **S.A.** — strongly altered rocks.

SAMPLE	Mineral	Fe^{2+}									Fe^{3+}			Fe^{3+}/Fe^{2+}
		QS_1 (mm/s)	IS_1 (mm/s)	A_{rel} (%)	QS_2 (mm/s)	IS_2 (mm/s)	A_{rel} (%)	QS_3 (mm/s)	IS_3 (mm/s)	A_{rel} (%)	QS_4 (mm/s)	IS_4 (mm/s)	A_{rel} (%)	
PYH–15 (L.A.)	Bt	2.67	1.02	43.5	2.31	1.00	46.5	1.14	0.72	2.1	0.62	0.35	7.9	0.086
PYH–9 (M.A.)	Bt	2.72	1.02	49.8	2.46	1.03	48.0	-	-	-	0.62	0.10	2.2	0.022
PYH–3 (M.A.)	Chl	2.67	1.02	77.7	2.02	0.91	13.0	-	-	-	0.62	0.10	9.3	0.103

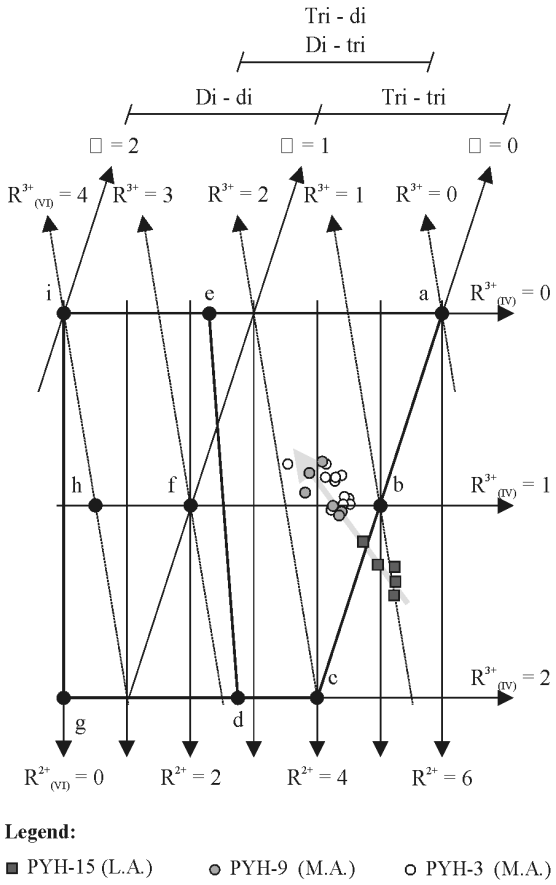

Fig. 7. General representation of chlorite chemical composition from the Pezinok Sb-Au deposit based on the octahedral cations R^{2+}, R^{3+}, tetrahedral cations $R^{3+(IV)}$ and vacancy in octahedral position (marked by □). The field confined by the thick line represents theoretically possible chemistry of chlorites. Explanations to isoline descriptions: $R^{3+(VI)} = 4$ represents four trivalent octahedral cations and $R^{3+(IV)} = 1$ represents one trivalent tetrahedral cations, etc. Points designated by letters represents the following general chemical composition of chlorites: **a** — $(R^{2+}_6)(R^{4+}_4)O_{10}(OH)_8$, **b** — $(R^{2+}_5R^{3+}_1)(R^{4+}_3R^{3+}_1)O_{10}(OH)_8$, **c** — $(R^{2+}_4R^{3+}_2)(R^{4+}_2R^{3+}_2)O_{10}(OH)_8$, **d** — $(R^{2+}_{2.8}R^{3+}_{2.8}□_{0.4})(R^{4+}_2R^{3+}_2)$ $O_{10}(OH)_8$, **e** — $(R^{2+}_2R^{3+}_{2.4}□_{1.2})$ $(R^{4+}_4)O_{10}(OH)_8$, **f** — $(R^{2+}_2R^{3+}_3□_1)(R^{4+}_3R^{3+}_1)O_{10}(OH)_8$, **g** — $(R^{3+}_{4.7}□_{1.3})$ $(R^{4+}_2R^{3+}_2)O_{10}(OH)_8$, **h** — $(R^{2+}_{0.5}R^{3+}_4□_{1.5})$ $(R^{4+}_3R^{3+}_1)O_{10}(OH)_8$, **i** — $(R^{3+}_4□_2)(R^{4+}_4)O_{10}(OH)_8$ (Wiewióra & Weiss 1990; Weiss 1991). The grey arrow shows increasing degree of hydrothermal alteration.

-substitution of Al by Si together with a decrease in interlayer occupancy on A site according to reaction (7). The content of octahedral Al ranges from 0.778 to 0.843 a.p. 11 oxygens and content of A site (K + Ca + Na) ranges from 0.905 to 0.964 a.p. 11 oxygens. The average formula is: $(K_{0.869}Ca_{0.056}Na_{0.014})(Al_{1.623}Ti_{0.018}Fe_{0.112}Mg_{0.302}Mn_{0.003}□_{0.942})(Si_{3.276}Al_{0.724})O_{10}(OH)_2$.

Illites from strongly altered rocks (see Fig. 10D) have a lower content of Fe_{tot} (0.020–0.065 a.p. 11 oxygens), whilst the content of Mg ranges from 0.024 to 0.187 a.p. 11 oxygens.

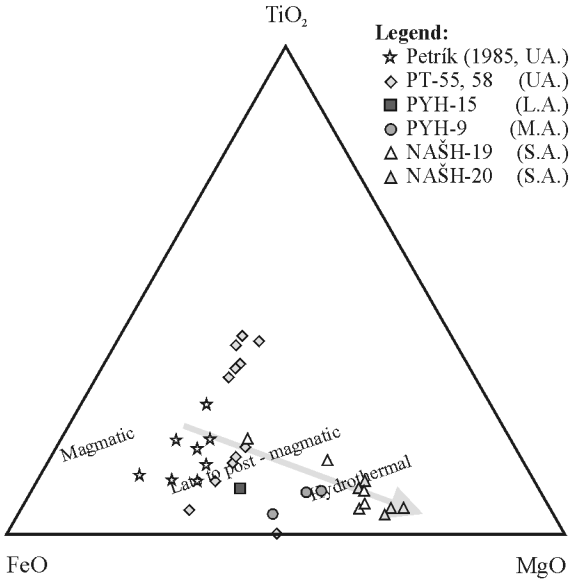

Fig. 8. Distinction between magmatic, post to late-magmatic and hydrothermal white K-mica from the Pezinok Sb-Au deposit by means of TiO_2, FeO and MgO (Miller et al. 1981). The grey arrow shows increasing degree of hydrothermal alteration.

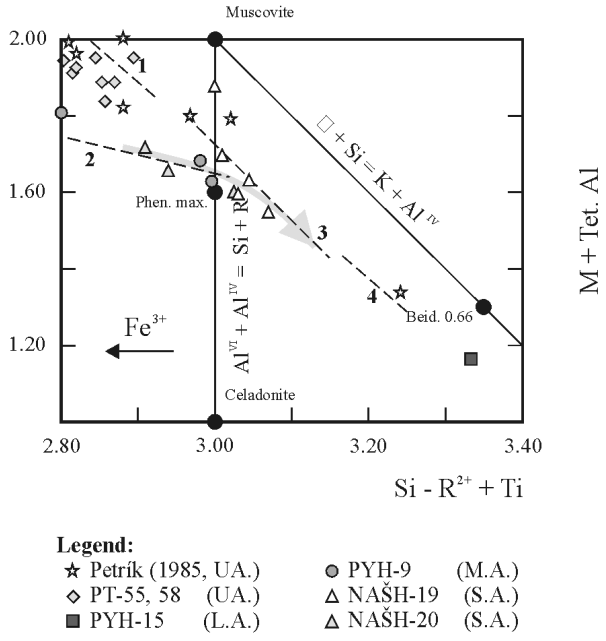

Fig. 9. Principal chemical characteristics of hydrothermal white K-micas from the Pezinok Sb-Au deposit. M + Al^{IV} vs. Si - R^{2+} + Ti. M = K + Na + 2. (Ca + Ba + Sr), R^{2+} = Fe + Mg + Mn. Plotted end-members (filled circles) are muscovite (Musc.), celadonite (Cela.), high-charge beidellite (Beid. 0.66), and phengite substitution maximum (Phen. max.), **1** — idioblastic muscovite, **2** — illite-phengitic muscovite, **3** — phengitic muscovite, **4** — illite (Piantone et al. 1994). The grey arrow shows increasing degree of hydrothermal alteration.

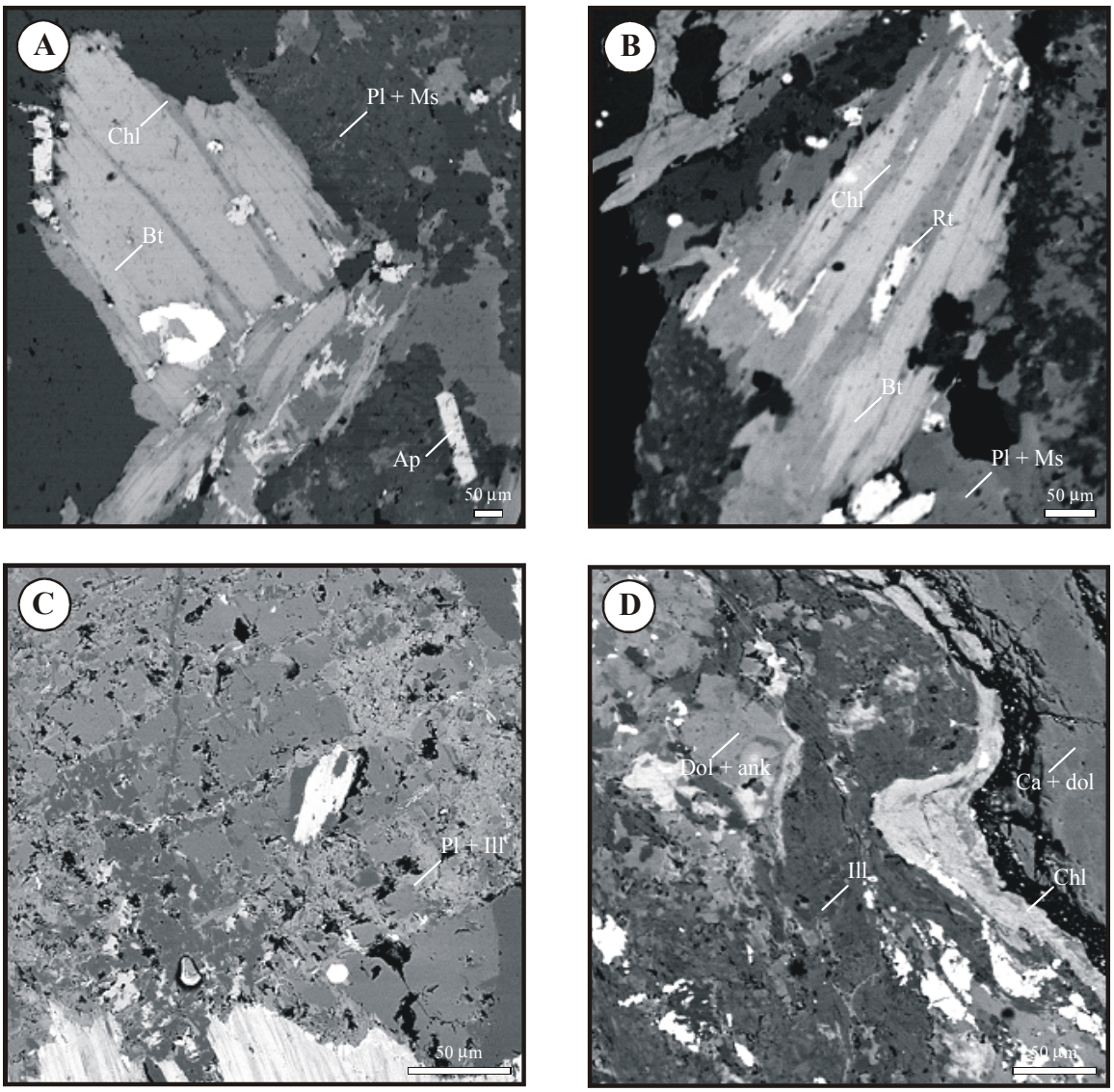

Fig. 10. Back scattered electron images of the thin polished section of phyllosilicates from altered granitoid rocks of the Pezinok Sb-Au deposit. **A** — Back scattered electron image of the thin polished section of chloritized biotites (less altered rocks), **B** — Back scattered electron image of the thin polished section of chloritized biotites (more altered rocks), **C** — Back scattered electron image of the thin polished section of altered plagioclases with illites and phengites (more altered rocks) and **D** — Back scattered electron image of the thin polished section of illites (strongly altered rocks). Legend: **Ank** — ankerite, **Ap** — apatite, **Bt** — biotite, **Ca** — calcite, **Dol** — dolomite, **Chl** — chlorite, **Ill** — illite, **Ms** — muscovite, **Pl** — plagioclase, **Rt** — rutile.

Content of Ti, which may indicate magmatic, postmagmatic or hydrothermal origin of micas (Miller et al. 1981) ranges from 0.005 to 0.019 a.p. 11 oxygens. These results are in compliance with the data for hydrothermal micas (see Fig. 8). The phengitic component (Brigatti et al. 2000) is very low and ranges from 0.02 to 0.14.

The main type of substitution involves formation of interlayer vacancies ($A_{-1}(Si_{+1}Al_{-1})$) according to reaction (7) where $\square^{A}$ is an interlayer vacancy in the A site (Konings et al. 1985, see Fig. 3D). This type of substitution leads to formation of illite $K_{0.65}Al_2\square Al_{0.65}Si_{3.35}O_{10}(OH)_2$ (Cathelineau & Izquierdo 1988) and later to the creation of pyrophylite endmember $Si_4Al_2O_{10}(OH)_2$. The content of K in samples from the PKV Sb-Au deposit, range from 0.770 to 0.926 a.p. 11 oxygens and it is close to ideal content of K in illite (Cathelineau & Izquierdo 1988). The present of illite has also been confirmed by X-ray study of clay material (see Table 2). Another important substitution is dioctahedral-trioctahedral substitution according to reaction (2) which causes octahedral vacancies ($\square^{VI}$ = 0.942–0.980 a.p. 11 oxygens).

These substitutions are combined with low Tschermak's substitution according to the reaction (1) where R^{3+} = Al, R^{2+} = Mg, Mn, Fe^{2+} (Velde 1965, 1967) and is confirmed by the low content of a phengitic component (0.02–0.14). The content of octahedral Al ranges from 1.777 to 1.970 a.p. 11 oxygens. The average formula is: $K_{0.845}(Al_{1.861}Ti_{0.010}Fe_{0.044}Mg_{0.128}\square_{0.957})(Si_{3.187}Al_{0.813})O_{10}(OH)_2$.

The chemical composition of the primary muscovites (Petrík 1985, ZK-8, ZK-49, ZK-50, ZK-51, ZK-53, ZK-54, ZK-60 and ZK-126 (Bratislava granitoid massif)) is analogous to the phengitic muscovites studied. These micas have Fe_{tot} content varying from 0.146 to 0.252 a.p. 11 oxygens, the con-

tent of Mg ranges from 0.084 to 0.126 a.p. 11 oxygens and the content Ti from 0.023 to 0.050 a.p. 11 oxygens. The phengitic component is 0.07–0.16. Our study of granitoid rocks from borehole PT-55, 58 (locality Trojárová) yielded similar conclusions. These samples have a content of Fe_{tot} (0.059–0.110 a.p. 11 oxygens) and of Mg (0.071–0.109 a.p. 11 oxygens). The phengitic component is 0.06–0.09 and the content of Ti is 0.019–0.080 a.p. 11 oxygens. The content of A site (K + Ca + Na) ranges from 0.930 to 0.999 a.p. 11 oxygens.

A more exact classification of single analyses according to Piantone et al. (1994) is shown in the M + Tet. Al vs. Si–R^{2+} + Ti diagram (see Fig. 9). Analyses from Petrík (1985) and borehole PT-55, 58 (locality Trojárová) lie in the field of muscovite, analyses from more altered granitoid rocks lie in the field of phengitic muscovite and analyses from strongly altered rocks lie in the field of illite-phengitic muscovite. No illites s.s. were found. Selected electron microprobe analyses of phengitic muscovites, illites and the percentage value of the phengitic component are given in Table 5.

Conclusions

The ratio of $Fe_{tot}/(Fe_{tot} + Mg)$, the rock-forming mineral assemblage and the multicationic $Q_3B_3F_3$ (de la Roche 1980) indicate that studied granitoid rocks are close to metaaluminous to peraluminous granodiorites of the Modra granitoid massif. These conclusions are not in compliance with Cambel & Vilinovič (1987). We consider that some granitoid bodies in the Pernek Unit (Putiš 1992) have a very close relationship to the Modra granitoid massif.

Biotites from altered granitoid rocks on Pezinok-Kolársky vrch Hill Sb-Au deposit belong to the phlogophite-annite series with the ratio $Fe_{tot}/(Fe_{tot} + Mg)$ = 0.44–0.55. Mg-biotites are the dominant type and can be classified as phlogopites ($Phl_{30.09-45.79}Ann_{26.67-36.00}Eas_{22.93-10.22}Sid_{20.31-8.02}$). Fe-biotites (annites, $Phl_{34.79-41.13}Ann_{39.20-46.39}Eas_{12.22-5.86}Sid_{13.79-6.62}$) are present in the more altered rocks. Electron microprobe analyses indicate that chemical composition is governed by substitutions (1), (2), (3), (4) and (7). Interlayer deficient occupancy of A site is probably caused by postmagmatic hydrothermal alteration and can be explained by substitution (7). From the change of chemical composition of biotites across alteration zones it is obvious that Al_2O_3 and K_2O were gradually removed, whereas FeO was added to the biotites. The relative amount of Fe^{3+} (below 10 %) indicates a decreasing degree of oxidation with an increasing degree of hydrothermal alteration. The Fe^{3+} is removed from biotites and during alteration is added to the chlorites. The reduction of Fe^{3+} into Fe^{2+} in the studied granitoid rocks is connected with the chemical nature of the wallrocks of the sulphidic PKV Sb-Au deposit.

The studied tri-trioctahedral chlorites are from clinochlore-chamosite isomorphic series and they originated from biotites. According to classification Wiewióra & Weiss (1990) or Weiss (1991), they can be divided into two groups: ferrous clinochlores (schematic formula $Mg_{34.39-36.32}Fe_{28.31-37.07}X_{24.02-35.39}$) and magnesium chamosites (schematic formula $Mg_{34.33-37.90}Fe_{34.76-39.32}X_{23.18-28.30}$). Ferrous clinochlore is the dominant type of chlorite. The chemical composition of chlorites is governed by dominant $FeMg_{-1}$-substitution and also by substitutions (2), (1) and (3). The content of impurities (K, Ca, Na) is very low.

White K-micas were formed mainly by alteration of alkali feldspars or plagioclases and can be divided into: phengitic muscovites and illites. Phengitc muscovites in the phengitic component (Brigatti et al. 2000) ranges from 0.17 to 0.25. The content of Ti is 0.016–0.020 a.p. 11 oxygens and indicates postmagmatic to hydrothermal origin (Miller et al. 1981). Content of interlayer occupancy (K + Ca + Na) ranges from 0.905 to 0.964 a.p. 11 oxygens and agrees with data from Konings et al. (1984), Piantone et al. (1994) and others. The chemical composition of phengitic muscovites is governed by substitutions (1), (2) and (7).

The phengitic component for illites is 0.02–0.14. The content of Ti (0.005–0.019 a.p. 11 oxygens) indicates hydrothermal origin (Miller et al. 1981). The content of K ranges from 0.770 to 0.926 a.p. 11 oxygens and agrees with data from Cathelineau & Izquierdo (1988), Aja et al. (1991a,b), Środroń & Eberl (1984) and others. The chemical composition of illites is governed by substitutions (7), (2) and (1). The change of chemical composition of white K-micas across alteration zones indicates that FeO and MgO were gradually removed, whereas Al_2O_3 and K_2O were added to phengitic muscovites and illites.

These conclusions agree with data from other Sb-Au deposits. Similar newly-formed minerals with chemical composition close to minerals studied and similar alteration processes, were described in France, for example: Haut Allier deposit (Bril & Beaufort 1989), Le Bourneix (Touray et al. 1989), Le Chatelet (Piantone et al. 1994) and also in the Dúbrava (Slovakia) Sb-Au deposit (Orvošová et al. 1998).

Acknowledgments: The financial support, obtained from Grant Agency for Science (VEGA No. 1/5218/98) as well as from the Geological Survey of the Slovak Republic (ŠGÚDŠ) No. 0599160, is gratefully acknowledged. We would like to thank Mgr. Daniel Ozdin (ŠGÚDŠ) for microprobe analyses of phyllosicates, RNDr. Ľubica Puškelová (Geological Institute of the Slovak Academy of Sciences) for X-ray diffraction analyses of clay material and Ing. Ignác Tóth (Department of Nuclear Physics and Technology of the Slovak University of Technology) for Mössbauer spectroscopy of phyllosilicates. Thanks also go to doc. RNDr. Pavel Fejdi, CSc. for reviewing an early version of the manuscript and to all reviewers.

References

Afifi A.M. & Essene E.J. 1988: MINFILE: A microcomputer program for storage and manipulation of chemical data on minerals. *Amer. Mineralogist* 73, 446–448.

Andráš P. 1983: Problems to the genesis of stibnite and gold mineralization at the deposit Pezinok. *Ph.D thesis, Manuscript, Geofond,* Bratislava, 1–154 (in Slovak).

Aja S.U., Rosenberg Ph.E. & Kittrick J.A. 1991: Illite equilibria: I. Phase relationships in the system K_2O-Al_2O_3-SiO_2-H_2O between 25 and 250 °C. *Geochim. Cosmochim. Acta* 55, 1353–1364.

Aja S.U., Rosenberg Ph.E. & Kittrick J.A. 1991: Illite equilibria in solutions: II. Phase relationships in the system K_2O-MgO-Al_2O_3-SiO_2-H_2O. *Geochim. Cosmochim. Acta* 55, 1365–1374.

Aubrecht J. & Hewitt D.A. 1980: Ti-substitution in synthetic Fe-bi-

otites. (abstr.) *Geol. Soc. Amer. Abstracts with Programs* 12, 377.
Bagdasarjan G.P., Gukasjan R.Ch., Cambel B. & Veselský J. 1982: The age of Malé Karpaty Mts granitoid rocks determined by Rb-Sr isochrone method. *Geol. Zbor. Geol. Carpath.* 33, 2, 131–140.
Bailey S.W. 1984: Crystal chemistry of true micas. In: Bailey S.W. (Ed.): Micas. *Rev. Mineralogy* 13, 13–60.
Bailey S.W. 1988: Chlorites: structure and crystal chemistry. In: Bailey S.W. (Ed.): Hydrous phyllosilicates (exclusive of micas). Mineralogical Society of America. *Rev. Mineralogy* 19, 347–403.
Brigatti M.F., Frigieri P., Ghezzo C. & Poppi L. 2000: Crystal chemistry of Al-rich biotites coexisting with muscovites in peraluminous granites. *Amer. Mineralogist* 85, 436–448.
Brill H. & Beaufort D. 1989: Hydrothermal alteration and fluid circulation related to W, Au, and Sb vein mineralizations, Haut Allier, Massif Central, France. *Econ. Geol.* 84, 2237–2251.
Cambel B. 1959: Hydrothermal deposits in the Malé Karpaty Mts, mineralogy and geochemistry of their ores. *Acta Geol. Geogr. Univ. Comen., Geol.* 3, 1–538.
Cambel B. & Petrík I. 1982: The West Carpathian granitoids: I/S classification and genetic implications. *Geol. Zbor. Geol. Carpath.* 33, 3, 255–267.
Cambel B. & Vilinovič V. 1987: Geochemistry and petrology of granitoids of Malé Karpaty Mts. *Veda*, Bratislava, 1–248 (in Slovak).
Cathelineau M. & Izquierdo G. 1988: Temperature — composition relationships of authigenic micaceous minerals in the Los Azufres geothermal system. *Contr. Mineral. Petrology* 100, 418–428.
Chovan M., Rojkovič I., Andráš P. & Hanas P. 1992: Ore mineralizations of the Malé Karpaty Mts (Western Carpathians). *Geol. Carpathica* 43, 5, 257–286.
Czamanske G.K. & Wones D.R. 1973: Oxidation during magmatic differentiation, Finnmarka Complex, Oslo area Norway, Part 2, The mafic silicates. *J. Petrology* 14, 349–380.
De Albuquerque C.A.R. 1973: Geochemistry of biotites from granitic rocks, Northern Portugal. *Geochim. Cosmochim. Acta* 37, 1779–1802.
De la Roche H. 1980: Granites chemistry through multicationic diagrams. *Sciences de la terre, Serie "Informatique Geologique" n.13, Proceedings of Gepic Meeting of 26–27 April 1979 Nancy-Vandoeuvre (France) — IGCP Project 154*, 65–88.
Dymek R.F. & Albee A.L. 1977: Titanium and aluminium in biotite from high-grade Archean gneisses, Lango, West Greenland. *Transactions, American Geophysical Union (EOS)*, 58, 525.
Dymek R.F. 1983: Titanium, aluminium and interlayer cation substitutions in biotite from high-grade gneisses, West Greenland. *Amer. Mineralogist* 68, 880–899.
Engel A.E.J. & Engel C. 1960: Progressive metamorphism and granitization of major paragneis, northwest Adirondack mountains, New York. Pt. 2. Mineralogy. *Geol. Soc. Amer. Bull.* 71, 1–58.
Eugster H.P. & Wones D.R. 1962: Stability relations of the ferruginous biotite, annite. *J. Petrology* 3, 82–125.
Forbers W.C. & Flowers M.F.J. 1974: Phase relations of titan-phlogophite, $K_2Mg_4TiAl_2Si_6O_{20}(OH)_4$: A refractory phase in the upper mantle? *Earth Planet. Sci. Lett.* 22, 60–66.
Foster M.D. 1960a: Layer charge relations in the dioctahedral and trioctahedral micas. *Amer. Mineralogist* 45, 383–398.
Foster M.D. 1960b: Interpretation of the composition of trioctahedral micas. *U.S. Geol. Sur. Profess. Pap.* 354 B, 11–60.
Foster M.D. 1962: Interpretation of the composition and a classification of the chlorites. *U.S. Geol. Sur. Profess. Pap.* 414 A, 1–33.
Hewitt D.A. & Aubrecht J. 1986: Limitations on the interpretation of biotite substitutions from chemical analyses of natural samples. *Amer. Mineralogist* 71, 1126–1128.
Joint Committee on Powder Diffraction Standards 1974: *Swarthmore*, Pennsylvania USA, 1–833.
Konings R.J.M., Boland J.N., Vriend S.P. & Jansen J.B.H. 1988: Chemistry of biotites and muscovites in the Abas granite, northern Portugal. *Amer. Mineralogist* 73, 754–765.
Lipka J. 1999: Mössbauer spectroscopy in mineralogy and petrology. In: Miglierini M. & Petridis D. (Eds.): Mössbauer spectroscopy in materials science. *Kluwer Academic Publishers*, Netherlands, 97–106.
Miller C.F., Stoddard E.F., Bradfish L.J. & Dollase W.A. 1981: Composition of plutonic muscovite: genetic implications. *Canad. Mineralogist* 19, 25–34.
Orvošová M., Majzlan J. & Chovan M. 1998: Hydrothermal alteration of granitoid rocks and gneisses in the Dúbrava Sb-Au deposit, Western Carpathians. *Geol. Carpathica* 49, 5, 377–387.
Petrík I. 1985: Biotite and muscovite in granitoid rocks of the Western Carpathians: geochemistry and petrogenetic importance. *Ph.D. thesis, Manuscript, Geofond*, Bratislava, 1–173 (in Slovak).
Petrík I., Broska I. & Uher P. 1994: Evolution of the Western Carpathian granite magmatism: age, source rock, geotectonic setting and relation to the Variscan structure. *Geol. Carpathica* 45, 5, 283–291.
Piantone P., Wu X. & Touray J.C. 1994: Zoned Hydrothermal Alteration and Genesis of the Gold Deposit at le Châtelet (French Massif Central). *Econ. Geol.* 89, 757–777.
Putiš M. 1992: Variscan and alpidic nappe structures of the Western Carpathian crystalline basement. *Geol. Carpathica* 43, 6, 369–380.
Rieder M., Cavazzini G., D'Yakonov Y.S., Frank-Kamenetski V.A., Gottardi G., Guggenheim S., Kovaľ P.V., Müller G., Neiva A.M.R., Radoslovich E.W., Robert J.L., Sassi F.P., Takeda M., Wiess Z. & Wones D.R. 1998: Nomenclature of the micas. *Canad. Mineralogist* 36, 41–48.
Shannon R.D. & Prewitt C.T. 1969: Effective ionic radii in oxides and fluorides. *Acta Crystallographica* B 25, 925–946.
Środroń J. & Eberl D.D. 1984: Illite. In: Bailey S.W. (Ed.): Micas. *Rev. Mineralogy* 13, 495–544.
Touray J.C., Marcoux E., Hubert P. & Proust D. 1989: Hydrothermal processes and ore-forming fluids in the Le Bourneix gold deposit, Central France. *Econ. Geol.* 84, 1328–1339.
Tracy R.J. & Robinson P.R. 1978: Metamorphic isograd mapping in central Massachusetts and the study of changing mineral compositions in metamorphism. *Geol. Soc. Amer. Abstracts with Programs* 10, 89.
Velde B. 1965: Phengite micas: synthesis, stability and natural occurrence. *Amer. J. Sci.* 263, 886–913.
Velde B. 1967: Si^{+4} content of natural phengites. *Contr. Mineral. Petrology* 14, 250–258.
Vivallo W. 1987: Early Proterozoic bimodal volcanism, hydrothermal activity, and massive sulphide deposition in the Boliden-Langdal area, Skellefte district, Sweden. *Econ. Geol.* 82, 440–456.
Weiss Z. 1991: Interpretation of chemical composition and X-ray diffraction patterns of chlorites. *Geol. Carpathica* 42, 2, 93–104.
Wiewióra A. & Weiss Z. 1990: Crystallochemical classification of phyllosilicates based on the unitied system of projection of chemical composition: II. The chlorite group. *Clay Miner.* 25, 83–92.
Wones D.R. 1963a: Phase equilibria of "ferriannite" $KFe^{2+}{}_3Fe^{3+}Si_3O_{10}(OH)_2$. *Amer. J. Sci.* 261, 581–596.
Wones D.R. 1963b: Physical properties of synthetic biotites on the join phlogophite-annite. *Amer. Mineralogist* 48, 1300–1321.
Wones D.R. & Eugster H.P. 1965: Stability of biotite: Experiment, theory, and application. *Amer. Mineralogist* 50, 1228–1272.
Zane A. & Weiss Z. 1988: A procedure for classification of rock-forming chlorites based on microprobe data. *Rend. Fis. Accad. Lincei* 9, 9, 51–56.